Intermittent Parathyroid Hormone Enhances Cancellous Osseointegration of a Novel Murine Tibial Implant

Xu Yang, MD, Benjamin F. Ricciardi, MD, Aleksey Dvorzhinskiy, BS, Caroline Brial, MEng, Zachary Lane, BS, Samrath Bhimani, BS, Jayme C. Burket, PhD, Bin Hu, MD, Alexander M. Sarkisian, MS, F. Patrick Ross, PhD, Marjolein C.H. van der Meulen, PhD, and Mathias P.G. Bostrom, MD

Investigation performed at the Hospital for Special Surgery, New York, NY

Background: Long-term fixation of uncemented joint implants requires early mechanical stability and implant osseointegration. To date, osseointegration has been unreliable and remains a major challenge in cementless total knee arthroplasty. We developed a murine model in which an intra-articular proximal tibial titanium implant with a roughened stem can be loaded through the knee joint. Using this model, we tested the hypothesis that intermittent injection of parathyroid hormone (iPTH) would increase proximal tibial cancellous osseointegration.

Methods: Ten-week-old female C57BL/6 mice received a subcutaneous injection of PTH (40 μg/kg/day) or a vehicle (n = 45 per treatment group) five days per week for six weeks, at which time the baseline group was killed (n = 6 per treatment group) and an implant was inserted into the proximal part of the tibiae of the remaining mice. Injections were continued until the animals were killed at one week (n = 7 per treatment group), two weeks (n = 14 per treatment group), or four weeks (n = 17 per treatment group) after implantation. Outcomes included peri-implant bone morphology as analyzed with micro-computed tomography (microCT), osseointegration percentage and bone area fraction as shown with backscattered electron microscopy, cellular composition as demonstrated by immunohistochemical analysis, and pullout strength as measured with mechanical testing.

Results: Preimplantation iPTH increased the epiphyseal bone volume fraction by 31.6%. When the data at post-implantation weeks 1, 2, and 4 were averaged for the iPTH-treated mice, the bone volume fraction was 74.5% higher in the peri-implant region and 168% higher distal to the implant compared with the bone volume fractions in the same regions in the vehicle-treated mice. Additionally, the trabecular number was 84.8% greater in the peri-implant region and 74.3% greater distal to the implant. Metaphyseal osseointegration and bone area fraction were 28.1% and 70.1% higher, respectively, in the iPTH-treated mice than in the vehicle-treated mice, and the maximum implant pullout strength was 30.9% greater. iPTH also increased osteoblast and osteoclast density by 65.2% and 47.0%, respectively, relative to the values in the vehicle group, when the data at post-implantation weeks 1 and 2 were averaged.

Conclusions: iPTH increased osseointegration, cancellous mass, and the strength of the bone-implant interface.

Clinical Relevance: Our murine model is an excellent platform on which to study biological enhancement of cancellous osseointegration.

Peer Review: This article was reviewed by the Editor-in-Chief and one Deputy Editor, and it underwent blinded review by two or more outside experts. It was also reviewed by an expert in methodology and statistics. The Deputy Editor reviewed each revision of the article, and it underwent a final review by the Editor-in-Chief prior to publication. Final corrections and clarifications occurred during one or more exchanges between the author(s) and copyeditors.

Disclosure: One or more of the authors received payments or services, either directly or indirectly (i.e., via his or her institution), from a third party in support of an aspect of this work. In addition, one or more of the authors, or his or her institution, has had a financial relationship, in the thirty-six months prior to submission of this work, with an entity in the biomedical arena that could be perceived to influence or have the potential to influence what is written in this work. No author has had any other relationships, or has engaged in any other activities, that could be perceived to influence or have the potential to influence what is written in this work. The complete **Disclosures of Potential Conflicts of Interest** submitted by authors are always provided with the online version of the article.

Cementless joint arthroplasty was developed to preserve bone stock, increase the ease of revision, and avoid complications related to cementation. The survival of uncemented implants requires osseointegration, which is the structural and functional connection between the bone and implant. Osseointegration requires initial implant stability after surgery, and early implant micromotion correlates with failure of total joint arthroplasty[1-6]. In total hip arthroplasty, cementless fixation of the femoral stem is achieved by direct contact with cortical bone, which has produced good clinical outcomes. In sharp contrast, the results of cementless total knee arthroplasty have been mixed, and the indications for its use are limited[7-12]. The tibial component in total knee arthroplasty relies on cancellous bone to achieve initial stability, and long-term failure of the bone-implant interface leading to aseptic loosening of the tibial component remains a major clinical challenge. The quantity and quality of cancellous bone vary widely among individuals. Many patients are not considered candidates for cementless total knee arthroplasty because of concerns about insufficient cancellous bone in the proximal part of the tibia[13-16]. Biological enhancement of cancellous bone quantity and osseointegration would provide one mechanism to improve the outcomes of cementless total knee arthroplasty.

Intermittent-injection recombinant human parathyroid hormone (iPTH) is the only anabolic agent approved by the U.S. Food and Drug Administration (FDA) to increase bone mineral density in osteoporotic patients. In previous animal models, iPTH enhanced implant osseointegration of nonphysiologically loaded cortical and cancellous bone in rabbits and rats[17-23]. These models fail to simulate the intra-articular environment and physiologic loading that accompany tibial cancellous fixation in total knee arthroplasty. To overcome the limitations of previous animal models, we developed a murine model that allows weight-bearing of the implant through the knee joint and relies exclusively on cancellous bone for support. We selected ten-week-old C57BL/6 mice for several reasons. First, this strain is used widely for the generation of transgenic and knockout animals for bone research[24]. In particular, numerous genetic variants are available, making these animals a useful tool for studying the molecular and cellular mechanisms underlying osseointegration. Second, iPTH reverses the bone loss accompanying ovariectomy of young C57BL/6 mice[25]. Thus, we used C57BL/6 mice to generate our preliminary data to assess whether perioperative iPTH enhances tibial cancellous osseointegration of our novel load-bearing uncemented implants.

Materials and Methods

Study Design

The experimental protocol was approved by our Institutional Animal Care and Use Committee. Ninety ten-week-old female C57BL/6 mice (Jackson Laboratory, Bar Harbor, Maine) were injected subcutaneously with either 40 μg/kg of PTH[25,26] (Amgen, Thousand Oaks, California) or a vehicle (0.9% saline solution) (n = 45 per treatment group) five days per week throughout the duration of the experiment (Fig. 1). The animals began receiving injections six weeks before surgery to avoid precluding any priming effects that iPTH may have on osseointegration of our implant. Injections were continued as part of a perioperative iPTH regimen until the animals were killed. One mouse in each group died during the first week of injections. After six weeks, six mice from each treatment group were killed to establish baseline data prior to surgery. The remaining animals underwent surgical implantation of a titanium implant in the right tibia. Mice from each treatment group were killed one, two, and four weeks after surgery (Fig. 1). All of the outcome measures were performed by investigators who were blinded to the treatment group and the duration of treatment.

Implant and Surgical Technique

See Appendix and Figure 2-A.

Microcomputed Tomography (MicroCT)

MicroCT scans (μCT 35; SCANCO Medical, Bassersdorf, Switzerland) were performed on all specimens at baseline (n = 6 per group), postoperative week 1 (n = 7 per group), week 2 (n = 14 per group), and week 4 (n = 17 per group), representing six, seven, eight, and ten weeks of iPTH therapy. A 6-μm voxel size, 55 kVp, 145 μA, and 0.36° rotation step (180° angular range) per view were used. Two volumes of interest—epiphyseal and metaphyseal cancellous bone—were examined (Fig. 2-B) for the baseline group. The area between these two volumes of interest was excluded to avoid the confounding effects of calcified cartilage from the growth plate. Additionally, this method allowed us to compare the effects of iPTH in periarticular (epiphyseal) bone and metaphyseal bone separately. We chose two other volumes of interest for the post-implantation groups killed at weeks 1, 2, and 4: (1) peri-implant (cancellous bone along the distal 500 μm of the stem) and (2) distal to the implant (cancellous bone in the 500-μm segment distal to the stem tip) (Fig. 2-B). Both volumes of interest were located within the metaphysis of the tibia to avoid including the growth plate. A 60-μm-thick volume around the edges of all implants was excluded to account for beam-hardening artifacts due to the metallic implant.

Mineralized tissue was segmented with use of global thresholds for each volume of interest (407.8 and 511.3 mg HA [hydroxyapatite] cm^{-3} for the epiphyseal and metaphyseal volumes of interest, respectively, in the baseline group and 681.4 and 348.9 mg HA cm^{-3} for the peri-implant and distal-to-implant volumes of interest, respectively, in the post-implantation groups). Bone volume fraction, trabecular number, trabecular thickness, and tissue mineral density were calculated.

Backscattered Electron Microscopy

Specimens collected at weeks 2 and 4 (n = 7 per group per time point) were fixed in 10% formalin for forty-eight hours and embedded in polymethylmethacrylate.

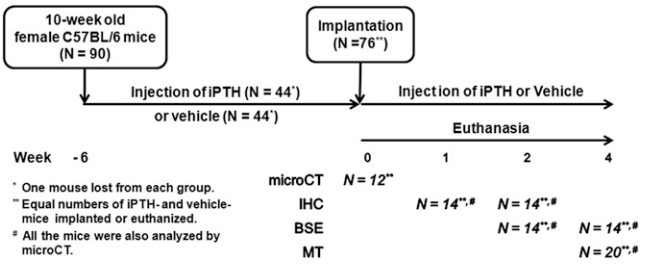

Fig. 1

Study design. Mice were pretreated for six weeks with iPTH (n = 45) or a vehicle (n = 45), and the same treatment modality was continued post-implantation for the remainder of the study in seventy-six of the mice. One mouse died in each treatment group during the early injection period. At week 0, a baseline group (n = 6 per treatment) was killed for microCT analysis. A tibial titanium implant was inserted into the proximal part of the tibia of the remaining mice, which were then killed at one, two, and four weeks after implantation surgery. The sample size for each outcome measure is shown. microCT= micro-computed tomography, IHC = immunohistochemistry, BSE = backscattered electron microscopy, and MT = mechanical testing.

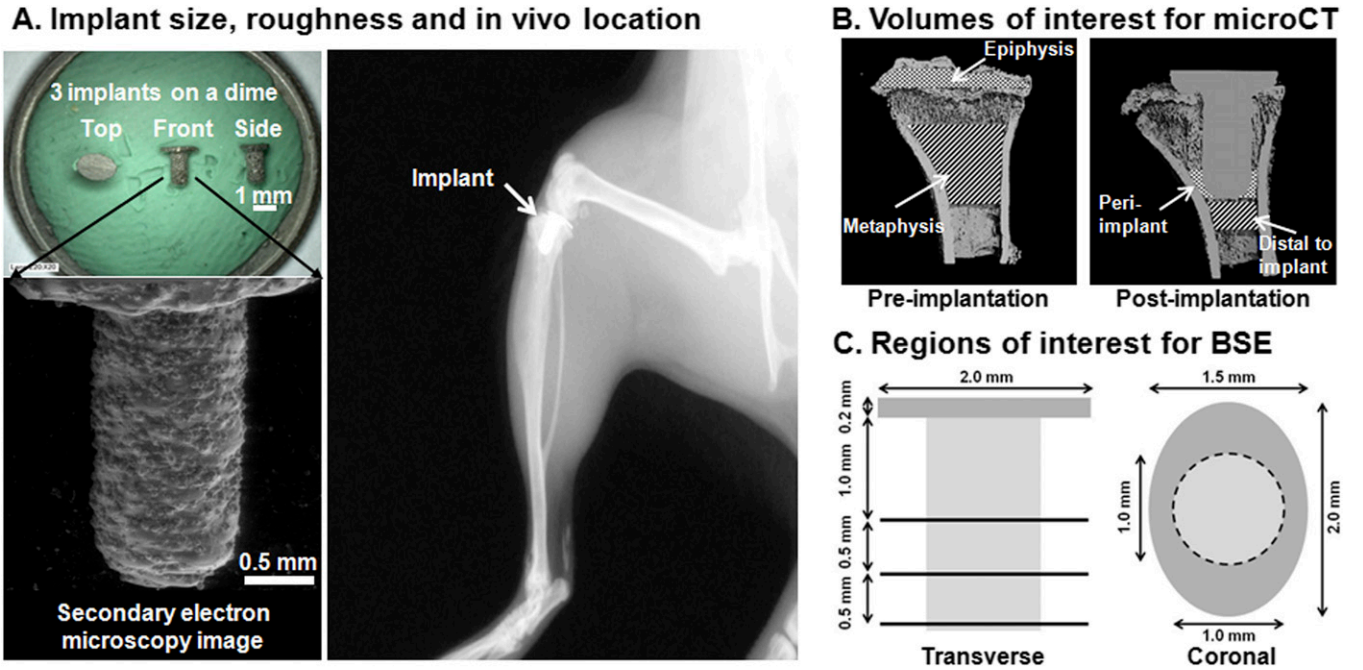

Fig. 2

Dimensions and use of the novel titanium tibial implant, which was manufactured with three-dimensional metal printing. **Fig. 2-A** Top left: Implants shown in top, front, and side views. The implants were placed on a dime for size comparison. Bottom left: Secondary electron microscopy image of the implant showing the roughened surface. Right: Lateral radiograph of a mouse knee with the tibial implant in situ. **Fig. 2-B** Volumes of interest for microCT measurements. Left: At baseline, epiphyseal and metaphyseal volumes of interest were analyzed separately, excluding calcified cartilage at the growth plate and all cortical bone. Right: At weeks 1, 2, and 4 post-implantation, peri-implant bone adjacent to the distal 500 μm of the implant and bone 500 μm distal to the implant were analyzed. **Fig. 2-C** Regions of interest for backscattered electron (BSE) microscopy. Left: Three transverse sections 0.5 mm apart were assessed and the results were averaged. Right: A coronal section on the midline of the plateau of the proximal 1.2 mm of the tibia was assessed.

Transverse sections perpendicular to the stem and coronal sections parallel to the stem were cut with a diamond saw (IsoMet 5000; Buehler, Lake Bluff, Illinois). The first transverse cut was made 1.2 mm distal to the top of the plateau; this was followed by two more cuts that were each displaced 0.5 mm from the preceding cut (Fig. 2-C). After imaging, a coronal cut was made on the proximal portion of the implant at the midline along the major axis. Thus, peri-implant metaphyseal bone was visualized on the three transverse sections and epiphyseal bone was visualized on the coronal sections. All cut surfaces were polished to a 1-μm surface finish with a polisher (EcoMet-III; Buehler) and imaged with backscattered electron microscopy (Quanta 600 Electron Microscope; FEI, Hillsboro, Oregon). The operating conditions were a 20-mm working distance, 30-kV accelerating voltage, 200-mm aperture setting, 0.78-A filament current, and 100-nA emission current. The osseointegration percentage, defined as the percentage of the total implant surface that had direct contact with bone, and the bone area fraction, defined as the percentage derived by dividing the area of bone by the total area within 200 μm of the implant, were assessed on the transverse and coronal sections (ImageJ; National Institutes of Health, Bethesda, Maryland). The results for the three transverse sections were averaged for each specimen.

Immunohistochemical Analysis

The specimens obtained at weeks 1 and 2 (n = 7 per group per time point) were fixed in 10% formalin for forty-eight hours and decalcified with use of 10% EDTA (ethylenediaminetetraacetic acid). The implants were then removed gently from the tibiae with minimal loss of tissue at the bone-implant interface[19], and the bone was embedded in paraffin. Transverse sections beginning 1 mm distal to the surface of the trimmed tibial plateau were cut serially. To analyze the peri-implant cellular responses to iPTH, immunohistochemical analysis was performed with procollagen I (1:50, SP1.D8; Developmental Studies Hybridoma Bank, University of Iowa, Iowa City, Iowa) as an osteoblast marker and cathepsin K (1:600)[27] as an osteoclast marker.

As previously described[19], sections were deparaffinized and rehydrated, endogenous peroxidase activity was blocked with 3% H_2O_2 for thirty minutes, and then a protein block solution (X0909; Dako, Carpinteria, California) was used for twenty minutes. Primary antibodies diluted in antibody diluent (S3022; Dako) were allowed to react overnight; this was followed by incubation with a biotinylated secondary antibody (1:200 E0464 [Dako] for procollagen I and 1:400 E0432 [Dako] for cathepsin K) for one hour. After fifteen minutes of incubation with avidin-biotin complex (VECTASTAIN [PK-6100]; Vector Laboratories, Burlingame, California), color was developed with diaminobenzidine (D5905; Sigma-Aldrich, St. Louis, Missouri) for twenty minutes. Sections were counterstained for ten seconds with methyl green for procollagen I and with hematoxylin for cathepsin K.

Images of sections were obtained at 20× magnification with a slide scanner (ScanScope Digital Scanner; Aperio Technologies, San Diego, California). Positive cells were counted with use of ImageJ. The total numbers of procollagen-I-positive and cathepsin-K-positive cells were manually counted, and the results were expressed as the osteoblast or osteoclast number/mm^2 in a circular area of interest 200 μm around the implant cavity.

Biomechanical Testing

The strength of the bone-implant interface was measured with pullout testing. Specimens obtained at week 4 (n = 10 per group) were wrapped in 0.9% saline-solution-soaked gauze and were frozen at −20°C. Before testing, each tibia was thawed to room temperature. The distal end was potted in polymethylmethacrylate. Bone at the proximal end was dissected with a number-11 scalpel blade to allow the clamp of a custom fixture[28] to hold the implant under its plateau. Care was

TABLE I Results of MicroCT of Cancellous Bone

	Mean (95% CI)		P Value (Student t Test or ANOVA)*		
	Vehicle Group	iPTH Group	Treatment	Duration	Treatment*Duration
Bone volume fraction *(%)*					
Epiphysis (baseline)	34.2 (32.3, 36.1)	45.0 (43.1, 46.8)	0.005	—	—
Metaphysis (baseline)	9.02 (8.55, 9.50)	8.60 (7.59, 9.61)	N.S.	—	—
Peri-implant			<0.001	N.S.	N.S.
Wk 1	21.9 (13.4, 30.3)	28.7 (25.4, 31.9)			
Wk 2	18.5 (14.5, 22.5)	35.1 (31.6, 38.6)			
Wk 4	15.3 (11.0, 19.6)	33.4 (29.0, 37.9)			
Distal to implant			<0.001	N.S.	0.015
Wk 1	23.9 (7.35, 40.5)	39.3 (33.6, 44.9)†			
Wk 2	12.7 (9.57, 15.9)	41.1 (36.0, 46.2)†			
Wk 4	9.75 (5.50, 14.0)‡	43.7 (37.7, 49.8)†			
Trabecular number *(mm^{-1})*					
Epiphysis (baseline)	8.19 (5.89, 10.5)	8.95 (7.60, 10.3)	N.S.	—	—
Metaphysis (baseline)	3.82 (3.68, 3.96)	3.77 (3.49, 4.04)	N.S.	—	—
Peri-implant			<0.001	0.018	N.S.
Wk 1	9.98 (6.34, 13.6)	14.7 (11.9, 17.5)			
Wk 2	8.47 (6.75, 10.2)	16.4 (15.0, 17.8)			
Wk 4§	6.17 (4.48, 7.85)	14.4 (12.6, 16.1)			
Distal to implant			<0.001	N.S.	N.S.
Wk 1	7.97 (3.05, 12.9)	9.78 (7.46, 12.1)			
Wk 2	4.19 (3.76, 4.61)	8.73 (7.05, 10.4)			
Wk 4	4.65 (3.73, 5.57)	10.8 (8.45, 13.2)			
Trabecular thickness *(μm)*					
Epiphysis (baseline)	57.5 (56.7, 58.3)	61.3 (58.3, 64.2)	0.030	—	—
Metaphysis (baseline)	43.6 (41.7, 45.4)	39.6 (36.6, 42.7)	0.031	—	—
Peri-implant			N.S.	<0.001	N.S.
Wk 1	28.0 (26.5, 29.6)	28.5 (26.8, 30.2)			
Wk 2	27.5 (26.1, 28.8)	29.0 (28.0, 30.0)			
Wk 4§#	32.4 (30.9, 33.9)	31.7 (30.4, 32.9)			
Distal to implant			<0.001	N.S.	N.S.
Wk 1	43.7 (36.2, 51.3)	44.8 (41.8, 47.7)			
Wk 2	40.4 (37.8, 42.9)	48.0 (46.1, 49.8)			
Wk 4	38.8 (33.9, 43.8)	47.7 (45.0, 50.5)			
Tissue mineral density *(mg HA cm^{-3})*					
Epiphysis (baseline)	951 (935, 968)	928 (920, 936)	0.013	—	—
Metaphysis (baseline)	913 (903, 924)	882 (862, 901)	0.013	—	—
Peri-implant			N.S.	0.001	N.S.
Wk 1	963 (955, 970)	961 (956, 967)			
Wk 2#	976 (970, 982)	969 (964, 973)			
Wk 4§	964 (960, 969)	965 (959, 971)			
Distal to implant			0.003	<0.001	N.S.
Wk 1	753 (723, 782)	735 (706, 763)			
Wk 2#	829 (816, 842)	803 (790, 815)			
Wk 4#	816 (800, 833)	805 (794, 816)			

*N.S. = not significant. †Significantly different from the value in the vehicle group at the same time point as shown by post hoc testing. ‡Significantly different from the value in the same treatment group at week 1 as shown by post hoc testing. §Significantly different from the value at week 2, independent of treatment, as shown by post hoc testing. #Significantly different from the value at week 1, independent of treatment, as shown by post hoc testing.

TABLE II Osseointegration and Bone Area Fraction Measured with Backscattered Electron Microscopy

	Mean (95% CI)		P Value (ANOVA)*		
	Vehicle Group	iPTH Group	Treatment	Duration	Treatment*Duration
Osseointegration *(%)*					
Metaphysis			0.019	N.S.	N.S.
Wk 2	45.6 (38.3, 52.9)	53.6 (46.5, 60.8)			
Wk 4	41.0 (16.8, 65.1)	57.3 (52.1, 62.5)			
Epiphysis			N.S.	N.S.	N.S.
Wk 2	17.4 (2.15, 32.7)	15.6 (0.381, 30.9)			
Wk 4	16.5 (5.16, 27.7)	22.8 (12.0, 33.6)			
Bone area fraction *(%)*					
Metaphysis			<0.001	N.S.	N.S.
Wk 2	32.2 (29.9, 34.5)	47.8 (44.5, 51.2)			
Wk 4	24.1 (13.0, 35.2)	48.4 (46.3, 50.6)			
Epiphysis			N.S.	N.S.	N.S.
Wk 2	40.3 (28.6, 52.0)	29.7 (16.5, 42.9)			
Wk 4	28.0 (17.1, 38.9)	30.7 (19.0, 42.3)			

*N.S. = not significant.

taken to minimize the amount of tissue removed and to not move the implant in the process[28]. The long axis of the implant was aligned with the axis of pullout loading. The implant was pulled out of the tibia at 0.03 mm/sec under displacement to failure with an EnduraTEC ELF 3200 system (Bose, Eden Prairie, Minnesota). Maximum pullout load (N) was calculated from the load-displacement curves.

Statistical Analysis

Baseline differences in microCT parameters and differences in mechanical testing data between treatment groups were assessed with Student t tests. Post-implantation differences in microCT, backscattered electron microscopy, and immunohistochemistry parameters, including effects of treatment, weeks after implantation, and their interaction, were evaluated with multifactor analysis of variance (ANOVA). If no significant interaction was present, only main effects are reported. The data at all of the post-implantation time points in each treatment group were averaged to calculate the difference between the two treatment groups when the difference was independent of the duration of treatment. Separate models were used to examine differences in microCT parameters in different volumes of interest. Post-hoc testing was performed with the Tukey method. $P < 0.05$ was considered to indicate significance. Results are presented as means and 95% confidence intervals (CIs). All results presented are significant unless stated otherwise.

Source of Funding

This study was supported by Grant UL1 TR000457 of the Clinical and Translational Science Center at Weill Cornell Medical College (X.Y.), the Eduardo A. Salvati Resident Research Grant (B.F.R.), and National Institutes of Health (NIH) Grant R01-AR056802.

Results

Preimplantation iPTH Increased Bone Volume and Trabecular Thickness in a Site-Specific Manner (Table I)

Six weeks of iPTH treatment increased the preimplantation epiphyseal cancellous bone volume fraction by 31.6% and epiphyseal trabecular thickness by 6.6% relative to the values

TABLE III Osteoblast and Osteoclast Densities Measured with Immunohistochemical Analysis

	Mean (95% CI)		P Value (ANOVA)*		
	Vehicle Group	iPTH Group	Treatment	Duration	Treatment*Duration
No. of osteoblasts/area *(mm^{-2})*			0.002	0.005	N.S.
Wk 1	406 (213, 599)	640 (402, 878)			
Wk 2	281 (162, 399)	495 (363, 627)			
No. of osteoclasts/area *(mm^{-2})*			0.038	0.047	N.S.
Wk 1	66.4 (26.0, 107)	71.4 (45.9, 96.9)			
Wk 2	69.9 (38.6, 101)	129 (86.2, 171)			

*N.S. = not significant.

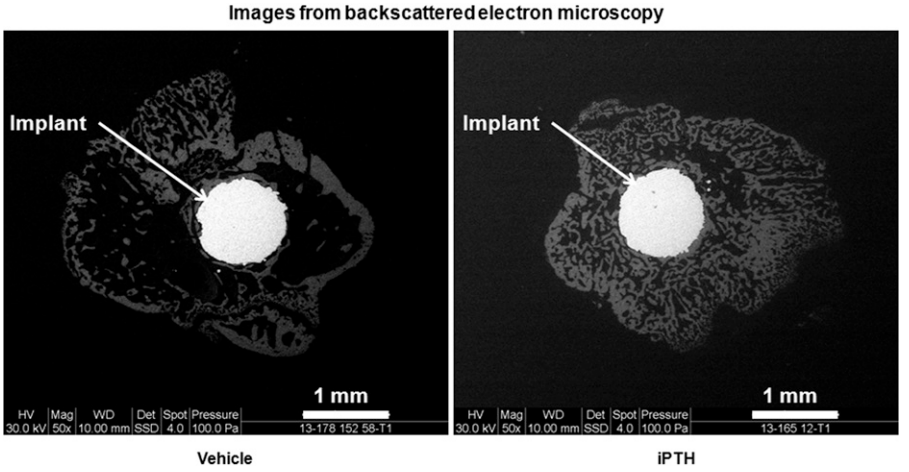

Fig. 3

Treatment with iPTH enhanced osseointegration and bone area fraction in the metaphyseal region, as shown by these representative backscattered electron microscopy images of the metaphyseal (transverse) region of vehicle and iPTH-treated mice at week 4 post-implantation.

for the vehicle control, whereas iPTH decreased the metaphyseal cancellous trabecular thickness by 9.2%. Preimplantation iPTH did not alter the trabecular number; however, it decreased tissue mineral density in both the epiphyseal and the metaphyseal region by 2.4% and 3.4%, respectively.

Peri-Implantation iPTH (Before and After Implantation) Augmented Bone Mass in Both the Peri-Implant and the Distal-to-Implant Region (Table I)

In the peri-implant region, iPTH treatment enhanced the bone volume fraction by 74.5% and the trabecular number by 84.8% without altering trabecular thickness when the data at the three post-implantation time points were averaged. The trabecular number decreased by 17.3% from two weeks to four weeks post-implantation, and this effect was independent of the treatment group. In the region distal to the implant region, iPTH increased bone volume fraction by 168%, trabecular number by 74.3%, and trabecular thickness by 14.3% when the data at the three post-implantation time points were averaged. The bone volume fraction was 64.4%, 224%, and 348% greater in the iPTH-treated mice at one, two, and four weeks post-implantation, respectively. The difference in bone volume fraction between

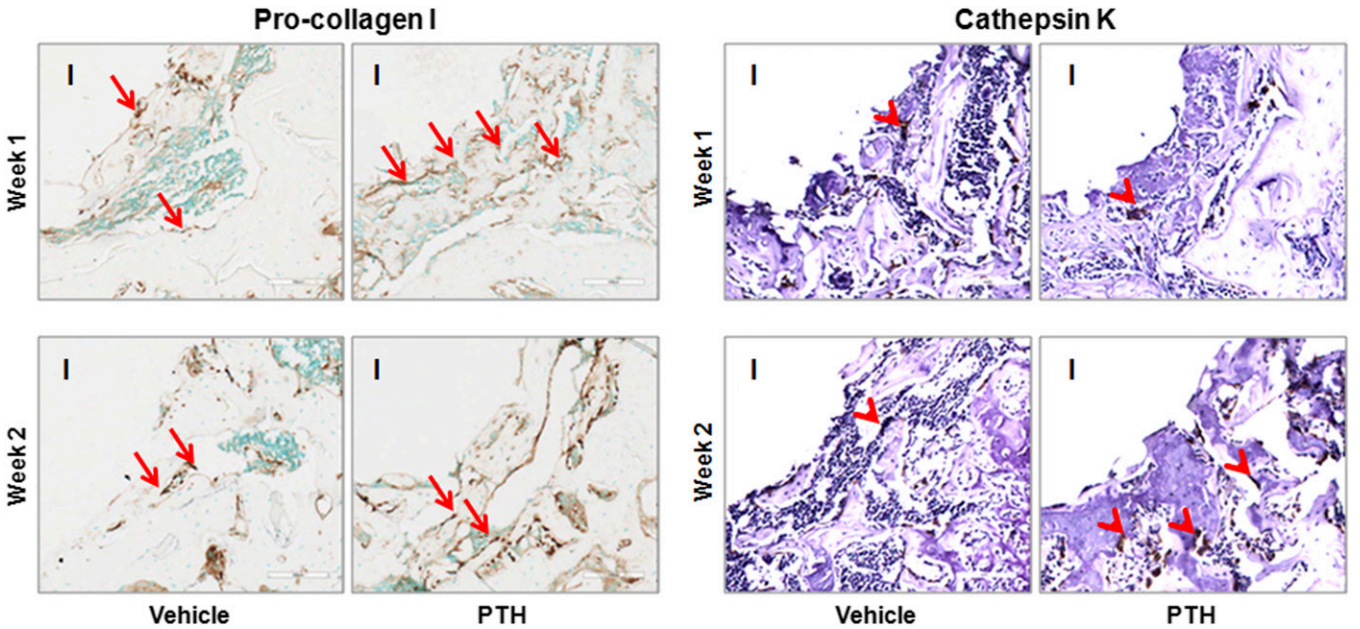

Fig. 4

Treatment with iPTH increased osteoblast and osteoclast density in the peri-implant region at weeks 1 and 2 post-implantation, as shown by these representative immunohistochemical staining images for osteoblasts (pro-collagen I) and osteoclasts (cathepsin K). I = empty space after the implant was withdrawn, arrow = osteoblast, and arrowhead = osteoclast.

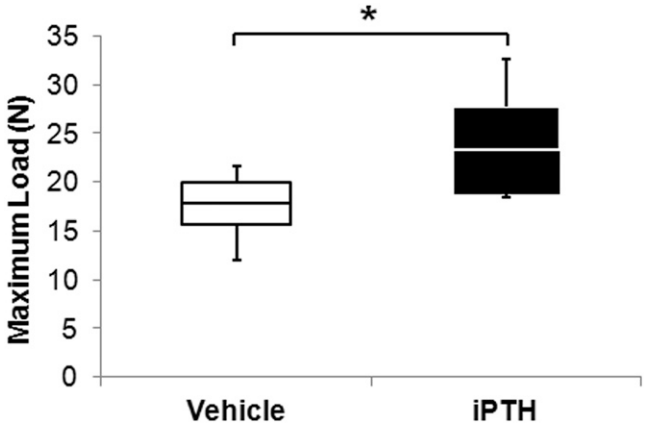

Fig. 5

Treatment with iPTH increased the maximum load to failure on pullout testing at week 4 post-implantation. This box and whisker plot shows the mean (line in the box), 95% confidence interval (bottom and top ends of the box), and minimum and maximum (bottom and top whiskers) of maximum load. *P < 0.05.

the two treatment groups was dependent on the duration of treatment. Treatment with iPTH decreased tissue mineral density by 2.29% in the region distal to the implant when the data at the three post-implantation time points were averaged. The bone volume fraction in this region decreased by 59.2% from one to four weeks in the vehicle-treated mice.

Peri-Implantation iPTH Enhanced Osseointegration and Bone Mass (Table II)

Treatment with iPTH increased the osseointegration percentage and bone area fraction by 28.1% and 70.1%, respectively, relative to the values in the vehicle-treated group, in the metaphyseal region along the implant stem (Fig. 3). In contrast, iPTH did not alter these two parameters in the coronal (epiphyseal) sections.

Peri-Implantation iPTH Increased Osteoblast and Osteoclast Number in the Peri-Implant Region (Table III)

Use of iPTH increased osteoblast density by 65.2% and osteoclast density by 47.0%, relative to the values in the vehicle-treated group, when the data at post-implantation weeks 1 and 2 were averaged (Fig. 4).

Peri-Implantation iPTH Increased Bone-Implant Interface Strength (Fig. 5)

The mean maximum pullout load at week 4 post-implantation in the iPTH group was 23.3 N (95% CI, 18.7 to 27.8 N), which was 30.9% higher than the value in the vehicle group (17.8 N [95% CI, 15.6 to 20.0 N]).

Discussion

Rapid and robust cancellous osseointegration of the proximal part of the tibial component is essential for the success of cementless total knee arthroplasties. Previous studies of in vivo models suggested that iPTH improves osseointegration[17-23,29-34]. Previous studies on osseointegration, however, had substantial limitations, including (1) use of large animals (rabbits, sheep, and dogs) with accompanying high cost, lower throughput[17,19,30,31,35-38], and greater humanitarian concerns compared with those related to small-animal models; (2) nonphysiologic implant placement such as in the medullary canal or extra-articular locations[18,20-22,32,39]; and (3) reliance on cortical bone support for stability[18,20-22,40]. In the present study, we used a newly developed murine model with an intra-articular titanium implant that was loaded through the knee joint and supported by the cancellous bone bed of the proximal part of the tibia. In this model, perioperative iPTH increased metaphyseal cancellous osseointegration.

The finding that iPTH enhanced bone formation within our titanium implant is consistent with the beneficial effects of iPTH therapy on osseointegration seen in other models[17-23,35]. In our study, an increase in trabecular number, as opposed to trabecular thickness, appeared to be the primary structural change resulting from iPTH in the peri-implant region compared with the distal region. Peri-implant trabecular thickness was similar between the vehicle and iPTH groups at all time points, suggesting that this morphologic parameter played less of a role in increasing the maximum failure load of the implant. In support of these observations, our previous study of rabbits showed an increase in the trabecular number, as opposed to trabecular thickness, as the primary morphologic change resulting from iPTH in combination with a surgical insult[19]. Pathologic bone states may have different responses to iPTH in the peri-implant region relative to normal bone. In contrast to our findings, a rat ovariectomy model showed increased trabecular thickness to be critical to improving bone-implant interface strength with iPTH[20]. The difference between iPTH actions in normal and pathologic bone states should be investigated in future studies.

Our data show that iPTH had distinct effects on preoperative bone mass and postoperative osseointegration in the epiphyseal and metaphyseal regions in young adult C57BL/6 mice. Preoperative iPTH significantly increased the epiphyseal but not the metaphyseal trabecular bone volume fraction. Similarly, Zhou et al. found that administration of iPTH at a dosage identical to the one used in our study (40 μg/kg/day) did not increase the trabecular bone volume fraction in the metaphyseal region of the proximal part of the tibia in C57BL/6 mice at seven weeks[25]. In contrast, sites with a high baseline trabecular bone volume, such as the vertebral body, did show a significantly increased bone volume fraction, suggesting that pretreatment trabecular bone density correlates with the iPTH effect.

Post-implantation, iPTH improved osseointegration and trabecular microarchitecture in the metaphyseal region. The increase in osteoblast and osteoclast density by two weeks suggests active remodeling in the peri-implant bone. The enhancement of osseointegration and the increase in peri-implant bone mass due to iPTH were pronounced and appeared to be independent of the impact of iPTH on trabecular bone remodeling in the preoperative state. Using a rabbit model, we previously showed improved osseointegration and greater osteoblast cell density in the setting of surgical trauma combined with iPTH treatment[19]. Collectively, these data suggest that synergy may exist between surgical trauma and iPTH treatment. An explanation for this result is that actively

remodeling surfaces may enhance the anabolic activity of osteoblasts in response to iPTH through the release of anabolic growth factors[41-44]. Surgical trauma stimulates a local healing response that may enhance these mechanisms of action[19].

Surprisingly, osseointegration in the epiphyseal region of the implant did not improve with iPTH treatment. One possible explanation is the exposure of this region to the joint cavity with synovial fluid access to the implant. In response to intra-articular injury, increased synovial fluid production of matrix metalloproteinases and inflammatory cytokines such as interleukin-6 and tumor necrosis factor-alpha can create an adverse biological healing environment[45-47]. Mechanical factors may also reduce osseointegration in the epiphyseal region. Fluctuations in fluid flow around an implant can induce osteoclastogenesis and contribute to bone resorption[48,49]. The distal part of the implant stem lies within the metaphysis and is not subject to the intra-articular environment, so this part of the stem may be less affected by the intra-articular environment and undergo better osseointegration. These spatially different osseointegration patterns may have clinical relevance, suggesting that proximal tibial plateau fixation needs to be supplemented by a stem to stimulate ingrowth and optimize early stability.

Our study has limitations. Given the size of the implant and bone, it was not possible to use instrument guides to trim the tibial plateau or adjust implant alignment. Using an operating microscope and landmarks such as the insertion of the posterior cruciate ligament and the blush of the tibial canal improved consistency in implant placement. The mice used the operatively treated leg normally throughout the postoperative period with no gait alterations after the immediate postoperative period (Video 1 [online]). This observation suggests that the mice were bearing weight; however, the force experienced by the implant has not been quantified.

In conclusion, iPTH treatment improved metaphyseal osseointegration and bone-implant interface strength in this novel physiologically loaded intra-articular murine model of tibial cancellous osseointegration. This model is a viable platform on which to study pharmacologic enhancement of the bone-implant interface and can be used in future studies to examine molecular mechanisms of osseointegration.

Appendix

Implant and Surgical Technique (Fig. 2-A)

The mouse implants were produced on a direct metal laser sintering system (EOSINT M 270; EOS Electro Optical Systems, Munich, Germany). The chemical composition of the Ti6Al4V powder was in accordance with ASTM F1472 and DIN (Deutsches Institut für Normung, translated into English as "The German Institute for Standardization") ISO (International Standards Organization) 5832-3. The powder was produced in an inert argon gas with use of a gas atomization process. The powder was spherical in shape with a median size (D50) of approximately 40 μm. The articulating surface of the implant was polished with 1200-grit (P2500) sandpaper, leading to a mean surface roughness of 8.4 μm. A minimum porosity of 39.5% was calculated with the assumption that there was a single layer of hexagonal close-packed 40-μm-diameter titanium spheres coating the implant stem. The dimensions of the smooth flat oval implant plateau were 2.0 mm for the major axis and 1.5 mm for the minor axis with a 0.2-mm thickness. The stem was 2.0 mm in length and 1.0 mm in diameter. The rough stem surface allowed bone ongrowth.

Surgery was carried out with the animal under general anesthesia induced with an intraperitoneal injection of ketamine (65 mg/kg) and acetylpromazine (2.5 mg/kg) with additional anesthesia (2% isoflurane, 2 L/min) administered with a nose cone as needed. With use of a sterile technique, an 8-mm medial parapatellar incision was made in the right knee. The longitudinal fibers of the quadriceps mechanism were divided medially, and the patella was dislocated laterally to expose the tibial plateau. With use of an operating microscope for visualization, the anterior cruciate ligament and menisci were resected. With use of a fine-tip burr, the articular cartilage and proximal epiphysis were removed to the level of the insertion of the posterior cruciate ligament to accommodate the implant. A 0.9-mm-diameter hole was created in the medullary canal with a high-speed drill. The implant was press-fit into the hole until the top was flush with the proximal part of the tibia. This press-fit approach was used to avoid early micromotion and decrease interface gaps[50-53]. A full range of motion of the knee was confirmed before the closure of the wound. The extensor mechanism and skin were closed in layers with resorbable suture. The mice were given analgesia (buprenorphine, 0.05 mg/kg subcutaneously) for the first forty-eight hours postoperatively. They bore full weight on the limb from the day of surgery onward and exhibited full unrestricted activity levels (Video 1 [online]). Immediately after the mice were killed, the right tibiae were dissected free of soft tissue with care taken to not disturb the tibial implant. Samples were fixed with 10% formalin or frozen at −20°C until processing for various outcome measures. ■

Xu Yang, MD
Benjamin F. Ricciardi, MD
Aleksey Dvorzhinskiy, BS
Caroline Brial, MEng
Zachary Lane, BS
Samrath Bhimani, BS
Jayme C. Burket, PhD
Alexander M. Sarkisian, MS
F. Patrick Ross, PhD
Mathias P.G. Bostrom, MD
Hospital for Special Surgery,
535 East 70th Street,
New York, NY 10021.
E-mail address for X. Yang: yangx@hss.edu

Bin Hu, MD
Department of Biomaterials and Biomimetics,
New York University College of Dentistry,
345 East 24th Street,
New York, NY 10010

Marjolein C.H. van der Meulen, PhD
Cornell University,
Ithaca, NY 14853

References

1. Chong DY, Hansen UN, Amis AA. Analysis of bone-prosthesis interface micromotion for cementless tibial prosthesis fixation and the influence of loading conditions. J Biomech. 2010 Apr 19;43(6):1074-80. Epub 2010 Mar 1.

2. Mjöberg B. Theories of wear and loosening in hip prostheses. Wear-induced loosening vs loosening-induced wear—a review. Acta Orthop Scand. 1994 Jun;65 (3):361-71.

3. Perren SM. Evolution of the internal fixation of long bone fractures. The scientific basis of biological internal fixation: choosing a new balance between stability and biology. J Bone Joint Surg Br. 2002 Nov;84(8):1093-110.

4. Ryd L, Albrektsson BE, Carlsson L, Dansgård F, Herberts P, Lindstrand A, Regnér L, Toksvig-Larsen S. Roentgen stereophotogrammetric analysis as a predictor of mechanical loosening of knee prostheses. J Bone Joint Surg Br. 1995 May;77 (3):377-83.

5. Mogensen B, Ekelund L, Hansson LI, Lidgren L, Selvik G. Surface replacement of the hip in chronic arthritis. A clinical, radiographic and roentgen stereophotogrammetric evaluation. Acta Orthop Scand. 1982 Dec;53(6):929-36.

6. Snorrason F, Kärrholm J. Primary migration of fully-threaded acetabular prostheses. A roentgen stereophotogrammetric analysis. J Bone Joint Surg Br. 1990 Jul;72(4):647-52.

7. Baker PN, Khaw FM, Kirk LM, Esler CN, Gregg PJ. A randomised controlled trial of cemented versus cementless press-fit condylar total knee replacement: 15-year survival analysis. J Bone Joint Surg Br. 2007 Dec;89(12):1608-14.

8. Berger RA, Lyon JH, Jacobs JJ, Barden RM, Berkson EM, Sheinkop MB, Rosenberg AG, Galante JO. Problems with cementless total knee arthroplasty at 11 years followup. Clin Orthop Relat Res. 2001 Nov;392:196-207.

9. Carlsson A, Björkman A, Besjakov J, Onsten I. Cemented tibial component fixation performs better than cementless fixation: a randomized radiostereometric study comparing porous-coated, hydroxyapatite-coated and cemented tibial components over 5 years. Acta Orthop. 2005 Jun;76(3):362-9.

10. Drexler M, Dwyer T, Marmor M, Abolghasemian M, Sternheim A, Cameron HU. Cementless fixation in total knee arthroplasty: down the boulevard of broken dreams - opposes. J Bone Joint Surg Br. 2012 Nov;94(11)(Suppl A):85-9.

11. Nakama GY, Peccin MS, Almeida GJ, Lira Neto OdeA, Queiroz AA, Navarro RD. Cemented, cementless or hybrid fixation options in total knee arthroplasty for osteoarthritis and other non-traumatic diseases. Cochrane Database Syst Rev. 2012;10:CD006193. Epub 2012 Oct 17.

12. Ranawat CS, Meftah M, Windsor EN, Ranawat AS. Cementless fixation in total knee arthroplasty: down the boulevard of broken dreams - affirms. J Bone Joint Surg Br. 2012 Nov;94(11)(Suppl A):82-4.

13. Labuda A, Papaioannou A, Pritchard J, Kennedy C, DeBeer J, Adachi JD. Prevalence of osteoporosis in osteoarthritic patients undergoing total hip or total knee arthroplasty. Arch Phys Med Rehabil. 2008 Dec;89(12):2373-4. Epub 2008 Nov 1.

14. Li MG, Nilsson KG. The effect of the preoperative bone quality on the fixation of the tibial component in total knee arthroplasty. J Arthroplasty. 2000 Sep;15(6): 744-53.

15. Sugita T, Umehara J, Sato K, Inoue H. Influence of tibial bone quality on loosening of the tibial component in total knee arthroplasty for rheumatoid arthritis: long-term results. Orthopedics. 1999 Feb;22(2):213-5.

16. Therbo M, Petersen MM, Varmarken JE, Olsen CA, Lund B. Influence of preoperative bone mineral content of the proximal tibia on revision rate after uncemented knee arthroplasty. J Bone Joint Surg Br. 2003 Sep;85(7):975-9.

17. Almagro MI, Roman-Blas JA, Bellido M, Castañeda S, Cortez R, Herrero-Beaumont G. PTH [1-34] enhances bone response around titanium implants in a rabbit model of osteoporosis. Clin Oral Implants Res. 2013 Sep;24(9):1027-34. Epub 2012 May 25.

18. Aspenberg P, Wermelin K, Tengwall P, Fahlgren A. Additive effects of PTH and bisphosphonates on the bone healing response to metaphyseal implants in rats. Acta Orthop. 2008 Feb;79(1):111-5.

19. Fahlgren A, Yang X, Ciani C, Ryan JA, Kelly N, Ko FC, van der Meulen MC, Bostrom MPG. The effects of PTH, loading and surgical insult on cancellous bone at the bone-implant interface in the rabbit. Bone. 2013 Feb;52(2):718-24. Epub 2012 May 18.

20. Gabet Y, Kohavi D, Voide R, Mueller TL, Müller R, Bab I. Endosseous implant anchorage is critically dependent on mechanostructural determinants of peri-implant bone trabeculae. J Bone Miner Res. 2010 Mar;25(3):575-83.

21. Gabet Y, Müller R, Levy J, Dimarchi R, Chorev M, Bab I, Kohavi D. Parathyroid hormone 1-34 enhances titanium implant anchorage in low-density trabecular bone: a correlative micro-computed tomographic and biomechanical analysis. Bone. 2006 Aug;39(2):276-82. Epub 2006 Apr 17.

22. Skripitz R, Aspenberg P. Implant fixation enhanced by intermittent treatment with parathyroid hormone. J Bone Joint Surg Br. 2001 Apr;83(3):437-40.

23. Takahata M, Schwarz EM, Chen T, O'Keefe RJ, Awad HA. Delayed short-course treatment with teriparatide (PTH(1-34)) improves femoral allograft healing by enhancing intramembranous bone formation at the graft-host junction. J Bone Miner Res. 2012 Jan;27(1):26-37.

24. Kimmel D. Animal models in osteoporosis research. In: Bilezikian JP, Raisz LG, Rodan GA, editors. Principles of bone biology. San Diego: Elsevier; 2002. p 1635-55.

25. Zhou H, Iida-Klein A, Lu SS, Ducayen-Knowles M, Levine LR, Dempster DW, Lindsay R. Anabolic action of parathyroid hormone on cortical and cancellous bone differs between axial and appendicular skeletal sites in mice. Bone. 2003 May;32 (5):513-20.

26. Reynolds DG, Takahata M, Lerner AL, O'Keefe RJ, Schwarz EM, Awad HA. Teriparatide therapy enhances devitalized femoral allograft osseointegration and biomechanics in a murine model. Bone. 2011 Mar 1;48(3):562-70. Epub 2010 Oct 13.

27. Zenger S, Hollberg K, Ljusberg J, Norgård M, Ek-Rylander B, Kiviranta R, Andersson G. Proteolytic processing and polarized secretion of tartrate-resistant acid phosphatase is altered in a subpopulation of metaphyseal osteoclasts in cathepsin K-deficient mice. Bone. 2007 Nov;41(5):820-32. Epub 2007 Jul 19.

28. Zhang L, Jia TH, Chong AC, Bai L, Yu H, Gong W, Wooley PH, Yang SY. Cell-based osteoprotegerin therapy for debris-induced aseptic prosthetic loosening on a murine model. Gene Ther. 2010 Oct;17(10):1262-9. Epub 2010 Apr 29.

29. Aspenberg P, Genant HK, Johansson T, Nino AJ, See K, Krohn K, García-Hernández PA, Recknor CP, Einhorn TA, Dalsky GP, Mitlak BH, Fierlinger A, Lakshmanan MC. Teriparatide for acceleration of fracture repair in humans: a prospective, randomized, double-blind study of 102 postmenopausal women with distal radial fractures. J Bone Miner Res. 2010 Feb;25(2):404-14.

30. Daugaard H, Elmengaard B, Andreassen T, Bechtold J, Lamberg A, Soballe K. Parathyroid hormone treatment increases fixation of orthopedic implants with gap healing: a biomechanical and histomorphometric canine study of porous coated titanium alloy implants in cancellous bone. Calcif Tissue Int. 2011 Apr;88(4): 294-303. Epub 2011 Jan 21.

31. Daugaard H, Elmengaard B, Andreassen TT, Baas J, Bechtold JE, Soballe K. The combined effect of parathyroid hormone and bone graft on implant fixation. J Bone Joint Surg Br. 2011 Jan;93(1):131-9.

32. Li YF, Li XD, Bao CY, Chen QM, Zhang H, Hu J. Promotion of peri-implant bone healing by systemically administered parathyroid hormone (1-34) and zoledronic acid adsorbed onto the implant surface. Osteoporos Int. 2013 Mar;24(3):1063-71. Epub 2013 Jan 8.

33. Neer RM, Arnaud CD, Zanchetta JR, Prince R, Gaich GA, Reginster JY, Hodsman AB, Eriksen EF, Ish-Shalom S, Genant HK, Wang O, Mitlak BH. Effect of parathyroid hormone (1-34) on fractures and bone mineral density in postmenopausal women with osteoporosis. N Engl J Med. 2001 May 10;344(19):1434-41.

34. Wu CC, Wei JC, Hsieh CP, Yu CT. Enhanced healing of sacral and pubic insufficiency fractures by teriparatide. J Rheumatol. 2012 Jun;39(6):1306-7.

35. Daugaard H, Elmengaard B, Andreassen TT, Lamberg A, Bechtold JE, Soballe K. Systemic intermittent parathyroid hormone treatment improves osseointegration of press-fit inserted implants in cancellous bone. Acta Orthop. 2012 Aug;83(4):411-9. Epub 2012 Aug 10.

36. Jensen TB, Bechtold JE, Chen X, Søballe K. Systemic alendronate treatment improves fixation of press-fit implants: a canine study using nonloaded implants. J Orthop Res. 2007 Jun;25(6):772-8.

37. Rong M, Zhu A, Guo Z, Zhou L, Li S, Lu H, Zhang X. The effects of early osseointegration in different implant sites in rabbit tibias. J Mater Sci Mater Med. 2013 Apr;24(4):959-65. Epub 2013 Feb 21.

38. Sumner DR, Turner TM, Urban RM, Virdi AS, Inoue N. Additive enhancement of implant fixation following combined treatment with rhTGF-beta2 and rhBMP-2 in a canine model. J Bone Joint Surg Am. 2006 Apr;88(4):806-17.

39. Yu X, Wang L, Jiang X, Rowe D, Wei M. Biomimetic CaP coating incorporated with parathyroid hormone improves the osseointegration of titanium implant. J Mater Sci Mater Med. 2012 Sep;23(9):2177-86. Epub 2012 May 26.

40. Dayer R, Badoud I, Rizzoli R, Ammann P. Defective implant osseointegration under protein undernutrition: prevention by PTH or pamidronate. J Bone Miner Res. 2007 Oct;22(10):1526-33.

41. Bonnet N, Conway SJ, Ferrari SL. Regulation of beta catenin signaling and parathyroid hormone anabolic effects in bone by the matricellular protein periostin. Proc Natl Acad Sci U S A. 2012 Sep 11;109(37):15048-53. Epub 2012 Aug 27.

42. Lindsay R, Cosman F, Zhou H, Bostrom MP, Shen VW, Cruz JD, Nieves JW, Dempster DW. A novel tetracycline labeling schedule for longitudinal evaluation of the short-term effects of anabolic therapy with a single iliac crest bone biopsy: early actions of teriparatide. J Bone Miner Res. 2006 Mar;21(3):366-73. Epub 2005 Nov 21.

43. Locklin RM, Khosla S, Turner RT, Riggs BL. Mediators of the biphasic responses of bone to intermittent and continuously administered parathyroid hormone. J Cell Biochem. 2003 May 1;89(1):180-90.

44. Ma YL, Zeng Q, Donley DW, Ste-Marie LG, Gallagher JC, Dalsky GP, Marcus R, Eriksen EF. Teriparatide increases bone formation in modeling and remodeling osteons and enhances IGF-II immunoreactivity in postmenopausal women with osteoporosis. J Bone Miner Res. 2006 Jun;21(6):855-64.

45. Higuchi H, Shirakura K, Kimura M, Terauchi M, Shinozaki T, Watanabe H, Takagishi K. Changes in biochemical parameters after anterior cruciate ligament injury. Int Orthop. 2006 Feb;30(1):43-7. Epub 2005 Dec 7.

46. Lohmander LS, Roos H, Dahlberg L, Hoerrner LA, Lark MW. Temporal patterns of stromelysin-1, tissue inhibitor, and proteoglycan fragments in human knee joint fluid after injury to the cruciate ligament or meniscus. J Orthop Res. 1994 Jan;12 (1):21-8.

47. Sun L, Zhou X, Wu B, Tian M. Inhibitory effect of synovial fluid on tendon-to-bone healing: an experimental study in rabbits. Arthroscopy. 2012 Sep;28(9):1297-305. Epub 2012 May 18.

48. Fahlgren A, Bostrom MP, Yang X, Johansson L, Edlund U, Agholme F, Aspenberg P. Fluid pressure and flow as a cause of bone resorption. Acta Orthop. 2010 Aug;81 (4):508-16.

49. Ferrier GM, McEvoy A, Evans CE, Andrew JG. The effect of cyclic pressure on human monocyte-derived macrophages in vitro. J Bone Joint Surg Br. 2000 Jul;82 (5):755-9.

50. Søballe K, Hansen ES, Brockstedt-Rasmussen H, Hjortdal VE, Juhl GI, Pedersen CM, Hvid I, Bünger C. Gap healing enhanced by hydroxyapatite coating in dogs. Clin Orthop Relat Res. 1991 Nov;272:300-7.

51. Bragdon CR, Burke D, Lowenstein JD, O'Connor DO, Ramamurti B, Jasty M, Harris WH. Differences in stiffness of the interface between a cementless porous implant and cancellous bone in vivo in dogs due to varying amounts of implant motion. J Arthroplasty. 1996 Dec;11(8):945-51.

52. Sandborn PM, Cook SD, Spires WP, Kester MA. Tissue response to porous-coated implants lacking initial bone apposition. J Arthroplasty. 1988;3(4): 337-46.

53. Dalton JE, Cook SD, Thomas KA, Kay JF. The effect of operative fit and hydroxyapatite coating on the mechanical and biological response to porous implants. J Bone Joint Surg Am. 1995 Jan;77(1):97-110.